Nonequilibrium Domain Pattern Formation in Mesoscopic Magnetic Thin Film Elements Assisted by Thermally Excited Spin Fluctuations

B. C. Choi and J. Ho
Department of Physics and Astronomy, University of Victoria, Victoria, BC, Canada

G. Arnup and M. R. Freeman
Department of Physics, University of Alberta, Edmonton, AB, Canada
(Received 3 March 2005; published 1 December 2005)

The dynamic behavior in the evolving pattern of thermally assisted, nonequilibrium domains in magnetic thin-film elements undergoing ultrafast 180° magnetization reversal was studied. Magnetization reversal enters a fully dynamic regime when the external field conditions are changed much faster than the sample is able to respond. The dynamic pathway develops a complexity not seen in quasistatic reversal but still retains a high level of order with well-developed dynamic domain patterns formed in response to subnanosecond transitions of the external applied magnetic field.

DOI: 10.1103/PhysRevLett.95.237211 PACS numbers: 75.60.Ch, 75.70.Ak, 75.70.Kw, 78.20.Ls

Self-organized pattern formation in systems driven away from equilibrium is a fascinating phenomenon observed in a wide variety of physical and chemical systems. Examples include the self-assembly of atoms on the surface of a solid and chemical waves in the Belousov-Zhabotinsky reaction [1–3]. The interplay of attractive and repulsive forces plays a key role in self-organization processes, but understanding specific pattern selection is a very challenging problem, and a unified description remains to be developed [4]. The possibility that a driven ferromagnet may be a model system for nonequilibrium pattern formation in dissipative systems has been debated on occasion in the literature [5,6].

In this Letter, we report picosecond time-resolved evolution of a nonequilibrium magnetic domain pattern of mesoscopic $Ni_{80}Fe_{20}$ thin-film elements. During the past few years, the study of magnetization reversal at the picosecond time scale in micro- and nanoscale magnets has attracted the attention of a number of research groups [7–10]. A recent focus has been on nearly uniform, precessional reversal or ''quasiballistic'' switching, which is fast, completely deterministic, and very promising for high speed memory applications [9]. Gerrits *et al.* [10] discussed a high degree of coherence in response to large angle excitation, with clear precessional oscillations of the magnetization observed. Importantly, the undesirable residual ringing after switching was suppressed completely through magnetic field pulse adjustment, and fast switching times of about 200 ps were achieved. In quasiballistic magnetization reversal, transverse magnetic field pulses are applied perpendicular to the initial direction of the magnetization. This field orientation results in a significant initial torque on the magnetization and initiates large angle precession.

Here we explore another limit of basic interest, in which there is little initial torque on the magnetization and thermal fluctuations play a large role in governing the subsequent evolution of the system. This regime has not been studied in detail and can be accessed via ultrafast imaging to reveal the spatially nonuniform dynamics. Recent non-time-resolved studies suggest that thermally excited magnons play a role in the onset of incoherent and chaotic switching [11].

A 15 nm thick polycrystalline $Ni_{80}Fe_{20}$ film was prepared by magnetron sputtering. During film deposition, a magnetic field was applied, resulting in an induced uniaxial anisotropy. Square elements of the size of $10\,\mu\text{m} \times 10\,\mu\text{m}$ were fabricated using electron beam lithography and lift-off. The patterned elements were made on a 20 μm wide by 300 nm thick gold transmission line that carried a fast current pulse [12]. The current created an in-plane switching field (H_s) of 24 kA/m in strength along the long axis of the sample, typically with 240 ps rise time and 10 ns duration. The current pulses were synchronously triggered by a mode-locked Ti:sapphire femtosecond laser (tuned to $\lambda = 780$ nm) at a 0.8 MHz repetition rate. Dynamic domain images were obtained using time-resolved scanning Kerr microscopy with a spatial resolution (Rayleigh criterion) of 800 nm. For the measurements, a so-called 180° dynamic magnetization reversal configuration was used, in which the sample was first magnetically saturated by an easy-axis static bias field ($H_l = 4.8$ kA/m) in the plane of the sample, and a switching field pulse ($H_s = 24$ kA/m) was then applied antiparallel to H_l in order to reverse the magnetization [12].

Consider first the spatiotemporal evolution of the easy-axis magnetization component in response to short magnetic pulses. Figure 1 shows dynamic domain images measured at selected time points after the application of the switching pulse. The contrast in the images reflects the local degree of magnetization reversal, with black areas (red in the online color version) corresponding to fully

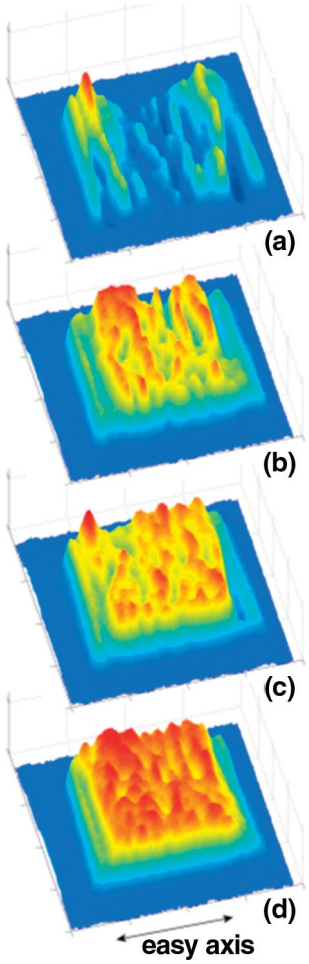

FIG. 1 (color online). Spatiotemporally resolved domain images representing the easy-axis magnetization component at selected time points after the onset of a magnetic switching field of 0.24 ns rise time (10%–90%). The 3D topography and color map both render the magnitude of the magnetic signal from unchanged (shown as white areas; blue in online version only) to fully reversed (shown as black areas; red in online version only). (a) 750; (b) 800; (c) 850; and (d) 900 ps.

reversed regions. The domain configurations show a complex spatial appearance, which is reminiscent of well-known labyrinth patterns. A well-developed labyrinth appears in the frame measured at 900 ps. We note that the qualitatively same behavior is observed in other samples with identical shape and dimension [13]. Emergence of the labyrinth can be seen from near the beginning of the reversal process. At the time delay of 750 ps, the magnetization reversal in progress at the ends of the platelet (along the field axis) is accompanied by the nucleation of branchlike fine structures in the interior regions. Labyrinth domain patterns evolve out of these nucleation sites, and, once a pattern forms, the completion of reversal is governed mainly by a gradual expansion of the initially reversed domains.

Another phenomenon appearing in the stroboscopic observation of these reversals far from equilibrium is modal oscillation of the dynamic domain pattern, shown in Fig. 2 for a series of frames captured at later times than those in Fig. 1. Some of the fine spatial structure has vanished before even the first cycle of precession is complete, but an alternating change of domain pattern contrast is observed clearly during the subsequent evolution, without significant changes of the pattern shape. Selecting frames according to the time traces in the inset [peak (a), dip (b), peak (c)], one sees an oscillation of the entire pattern superimposed upon the completion of the magnetization reversal. The selected domain pattern is maintained, while the remaining excess Zeeman energy introduced by the applied switching field is damped from the precessional magnetization motion.

The most interesting question is how this complex spatiotemporal structure arises. In order to shed light on this, we map out the transition from quasistatic to dynamic behavior by varying the rise time of the magnetic switching pulse. The upper panel in Fig. 3 shows the temporal evolution of the magnetization at the center of the same $10 \times 10\ \mu\mathrm{m}^2$ element, when driven by magnetic pulses with rise times $t_{\mathrm{rise}} = 8.6$, 5.1, 2.8, and 0.24 ns. All traces show the change of magnetization from one saturated state to another, with the magnetic response manifesting additional delay at longer pulse rise times, and with oscillations following the primary switch for all but the slowest excitation [14,15]. The bottom panel in Fig. 3 shows characteristic domain patterns imaged at the time points corresponding to 70% of the full M_x-intensity change. The situation for slow switching is very different from the fast case ($t_{\mathrm{rise}} = 0.24$ ns); for example, at $t_{\mathrm{rise}} = 5.1$ and 8.6 ns,

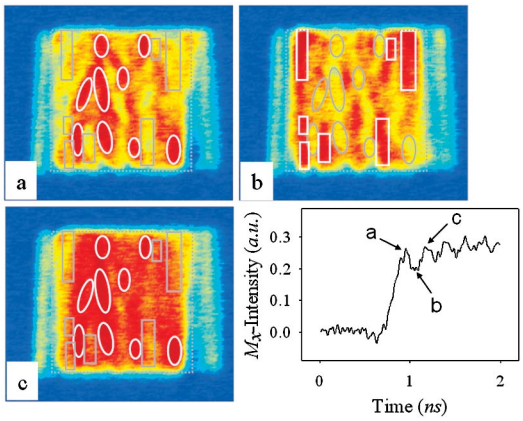

FIG. 2 (color online). Comparing spatiotemporally resolved domain images measured at the peaks (a) and (c) and dip (b) during magnetization oscillation. Through a cycle of oscillations, the already fully reversed regions at the oscillation peak (a) simply turn into not-fully reversed regions at the dip (b). In the next oscillation peak (c), one observes the same pattern with progressing reversal. Inset: Temporal evolution of the in-plane magnetization component measured at the center of the sample.

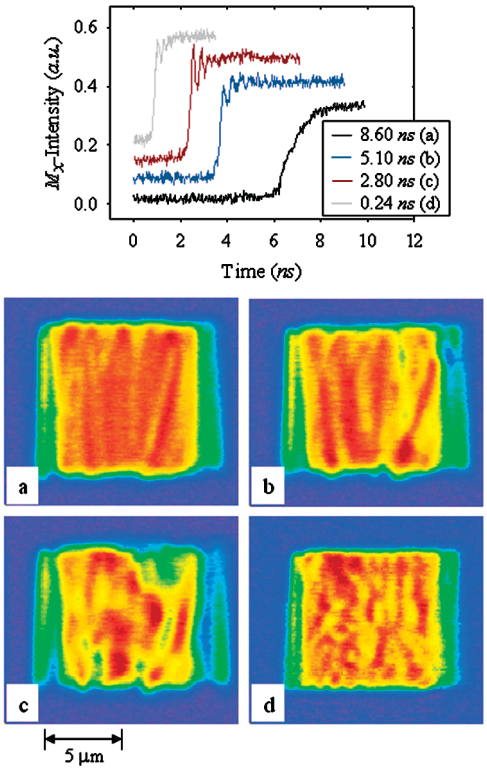

FIG. 3 (color online). (Top panel) Time traces of the magnetization at the center of the element, when excited by magnetic field pulses of different rise time [(a) 8.6, (b) 5.1, (c) 2.8, and (d) 0.24 ns]. Magnetic responses show additional delay with increasing rise time, with oscillations following the primary switch. (Bottom panel) Dynamic domain patterns revealed as a function of the magnetic pulse rise time. The spontaneous domain configuration is sensitively dependent on the switching speed.

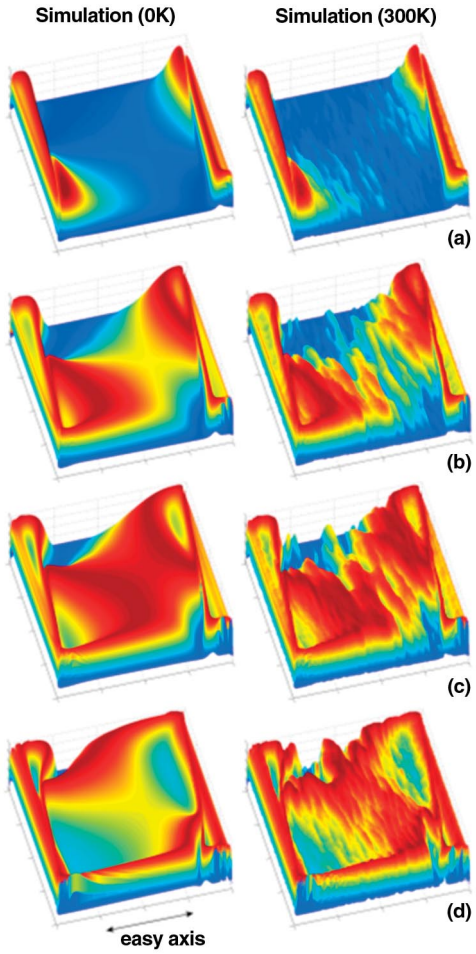

FIG. 4 (color online). Comparing domain configurations simulated at 0 and 300 K. The experimentally observed faint branchlike fine structure formed in the initial state of the magnetization reversal is well reproduced in the modeling, when carried out at 300 K. (a) 760; (b) 800; (c) 820; and (d) 860 ps.

the labyrinth domain pattern is no longer observed, and, instead, the domain configuration has a more regular character in which stripe domains predominate. It is in acceleration of the switching process well beyond the quasistatic limit that the more intricate structure develops.

In order to better understand the physical origin of the observed complex domain configuration, micromagnetic modeling based on the Landau-Lifshitz-Gilbert (LLG) equation was carried out, both with and without a Langevin term to represent thermal fluctuations [16]. Figure 4 shows a comparison of domain configurations simulated at (a) 0 and (b) 300 K. The modeling at 0 K reproduces some characteristics of the observed domain images, in which the magnetization reversal initiated at the element edges propagates towards the sample center. It also exhibits the qualitative characteristic of strong spatiotemporal oscillations observed in Fig. 2. Much better agreement with experiment is found by the modeling corresponding to a 300 K sample temperature. In particular, the experimentally observed faint branchlike fine structure formed in the initial stages of the magnetization reversal becomes clearly visible in the modeling, when carried out at 300 K. The evolution of the simulated domain configurations reveals that the complex domain structures evolve out of these fine structures, in agreement with experimental observations.

From this comparison, we conclude that the complex domain patterns are activated through the thermal fluctuations. We note that we can stochastically treat thermal fluctuations, since the characteristic time of thermally excited spin fluctuations is of the order of 10^{-13} s at room temperature and is much smaller than the response time of the magnetization, which is on the order of 10^{-9} s [17]. Thermally activated spin fluctuations quickly modulate each other via the exchange interaction and form local in-phase regions, which are manifested as the faint branchlike fine structure formed in the initial state of the magnetization reversal. This mechanism can be extended to the description for the systematic evolution of the domain patterns to progressively faster switching fields (Fig. 3).

In the case of relatively slow switching, e.g., $t_{\text{rise}} = 8.6$ ns, the thermally excited spins modulate long enough to create long stripe patterns [Fig. 3(a)], while complete stripe patterns cannot be formed for $t_{\text{rise}} = 0.24$ ns due to the limited time for completing modulation across the sample. Instead, labyrinthlike patterns, which are irregular-shaped regions due to uncompleted modulation processes, appear. Since such modulation is mediated by the exchange interaction of precessing spins, the characteristic time of modulation is given by the ferromagnetic resonance frequency, which is in the range of a few gigahertz in typical ferromagnetic materials. The characteristic spin modulation time can, therefore, be estimated to lie in the range below 1 ns. This is consistent with our experimental observations, where the characteristic stripe length scale reduces with increasing switching speed. Consequently, the appearance of complex domain pattern formation becomes more pronounced as the switching rate of the field increases towards $(0.24\ \text{ns})^{-1}$.

In conclusion, the thermal origin of complex dynamic domain pattern formation in nonequilibrium magnetic systems with mesoscopic length scales has been elucidated. An increasing complexity in the spatial structure of the evolution is found to accompany the increasing switching speed, when a ferromagnetic element is driven by progressively faster reversing fields applied antiparallel to the initial magnetization direction. This is in contrast to the case of quasiballistic switching, where a nearly uniform torque is applied to the entire magnetization and thermal nucleation is unimportant. As reversal rates approach the characteristic precession frequencies of spin fluctuations, the thermal energy can boost the magnetization into local configurations which are completely different from those experienced during quasistatic reversal. The sensitive dependence of the spatial pattern on switching speed can be understood in terms of a dynamic exchange interaction of thermally excited spins; the coherent modulation of the spins is strongly dependent on the rise time of switching pulses. When superimposed upon the overall nonuniform nonequilibrium energy landscape of the switching magnetization, the resulting fine spatial structure can be quasideterministic and yield patterns readily apparent to stroboscopically averaged ultrafast imaging. At an empirical level, the results suggest additional phenomena, which should be borne in mind in the quest for higher data rates in magnetic information technologies, from hard drives to spintronic devices.

We gratefully acknowledge support from the NSERC of Canada, the CIAR, Alberta Informatics Circle of Research Excellence, and the CRC program. The samples were produced at the University of Alberta NanoFab. We thank G. Nunes, F. Marsiglio, and F. Khanna for valuable discussions on various aspects of the experiments.

[1] R. Plass *et al.*, Nature (London) **412**, 875 (2001).
[2] M. Seul and D. Andelman, Science **267**, 476 (1995).
[3] P. Ball, *The Self-Made Tapestry: Pattern Formation in Nature* (Oxford University Press, Oxford, 1999).
[4] M. C. Cross and P. C. Hohenberg, Rev. Mod. Phys. **65**, 851 (1993).
[5] P. W. Anderson, in *Order and Fluctuations in Equilibrium and Nonequilibrium Statistical Mechanics*, edited by G. Nicolis, G. Dewel, and J. W. Turner (Wiley, New York, 1981), p. 289.
[6] T. Plefka, Phys. Rev. Lett. **75**, 144 (1995).
[7] W. K. Hiebert *et al.*, J. Appl. Phys. **93**, 6906 (2003).
[8] Th. Gerrits *et al.*, Nature (London) **418**, 509 (2002).
[9] H. W. Schumacher *et al.*, Phys. Rev. Lett. **90**, 017204 (2003).
[10] Th. Gerrits *et al.*, IEEE Trans. Magn. **38**, 2484 (2002).
[11] I. Tudosa *et al.*, Nature (London) **428**, 831 (2004).
[12] B. C. Choi and M. R. Freeman, in *Nonequilibrium Spin Dynamics by Time-Resolved Magneto-Optical Kerr Microscope*, edited by B. Heinrich and J. A. C. Bland, Ultrathin Magnetic Structures Vol. IV (Springer Verlag, Berlin, 2004).
[13] The domain patterns in various samples show slightly different fine structures but can still be characterized as the complex labyrinthlike structure. The slight difference in the patterns is a consequence of the variation of the demagnetization fields as a result of differences in local defects, edge smoothness, and thickness.
[14] B. C. Choi *et al.*, Phys. Rev. Lett. **86**, 728 (2001).
[15] Y. Acremann *et al.*, Science **290**, 492 (2000).
[16] M. R. Scheinfein, LLG Micromagnetic Simulator™ (http://llgmicro.ome.mindspring.com).
[17] W. F. Brown, Jr., Phys. Rev. **130**, 1677 (1963).